



DnaJ, a promising vaccine candidate against *Ureaplasma urealyticum* infection

Fangyi Guo^{1,2,3} · Yanhong Tang⁴ · Wenjun Zhang^{1,3} · Hongxia Yuan¹ · Jing Xiang¹ · Wenyong Teng¹ · Aihua Lei² · Ranhui Li² · Guozhi Dai^{1,3}

Received: 17 May 2022 / Revised: 20 September 2022 / Accepted: 5 October 2022
© The Author(s), under exclusive licence to Springer-Verlag GmbH Germany, part of Springer Nature 2022

Abstract

Ureaplasma urealyticum (*U. urealyticum*, Uu) is a common sexually transmitted pathogen that is responsible for diseases such as non-gonococcal urethritis, chorioamnionitis, and neonatal respiratory diseases. The rapid emergence of multidrug-resistant bacteria threatens the effective treatment of Uu infections. Considering this, vaccination could be an efficacious medical intervention to prevent Uu infection and disease. As a highly conserved molecular chaperone, DnaJ is expressed and upregulated by pathogens soon after infection. Here, we assessed the vaccine potential of recombinant Uu-DnaJ in a mouse model and dendritic cells. Results showed that intramuscular administration of DnaJ induced robust humoral- and T helper (Th) 1 cell-mediated immune responses and protected against genital tract infection, inflammation, and the pathologic sequelae after Uu infection. Importantly, the DnaJ protein also induced the maturation of mouse bone marrow-derived dendritic cells (BMDCs), ultimately promoting naïve T cell differentiation toward the Th1 phenotype. In addition, adoptive immunization of DnaJ-pulsed BMDCs elicited antigen-specific Immunoglobulin G2 (IgG2) antibodies as well as a Th1-biased cellular response in mice. These results support DnaJ as a promising vaccine candidate to control Uu infections.

Key points

- A novel recombinant vaccine was constructed against *U. urealyticum* infection.
- Antigen-specific humoral and cellular immune responses after DnaJ vaccination.
- Dendritic cells are activated by Uu-DnaJ, which results in a Th1-biased immune response.

Keywords Recombinant vaccine, · DnaJ, · *Ureaplasma urealyticum*, · Heat shock proteins, · Dendritic cells

Introduction

Ureaplasma urealyticum is a prevalent sexually transmitted pathogen that is commonly found in the genitourinary tract of both males and females (Sweeney et al. 2017). These organisms are

spherical or coccobacillus-shaped bacteria belonging to the class Mollicutes, a group of no cell wall bacteria whose evolution is from Gram-positive ancestors. The lack of a cell wall prevents Uu from staining by Gram stain and is responsible for their pleomorphic form (Kokkayil and Dhawan 2015). Epidemiological studies suggest that as many as 80% of pregnant women can be considered colonized with Uu in the mucosal surfaces of the vagina (Iwasaka et al. 1986; Silwedel et al. 2020). Furthermore, Uu can be isolated from the umbilical cord blood samples taken from 23% of infants born prematurely (Goldenberg et al. 2008; Rittenschober-Böhm et al. 2018; Silwedel et al. 2020). Noteworthy, Uu infection is frequently asymptomatic and chronic with clinical manifestations (Glass et al. 2000). However, in some individuals, Uu causes non-gonococcal urethritis, atypical neonatal respiratory diseases, chorioamnionitis, pre-term premature rupture of membranes, intraventricular haemorrhage, hyperammonaemia, and cerebral oedema (Taylor-Robinson 2017; Triantafilou et al. 2013; Sweeney et al. 2017). Moreover, this sexually transmitted

✉ Ranhui Li
Ranhui81@163.com

✉ Guozhi Dai
daigz008@126.com

¹ Center of Medical Laboratory, The First People's Hospital of Chenzhou, Chenzhou, China

² Pathogenic Biology Institute, Hengyang Medical School, University of South China, Hengyang, China

³ Center of Medical Laboratory, Affiliated the First People's Hospital of Chenzhou of University of South China, Chenzhou, China

⁴ State Key Laboratory of Respiratory Diseases, Guangzhou Medical University, Guangzhou, China

bacterium is resistant to several antibiotics, including levofloxacin, ciprofloxacin, tetracycline, erythromycin, azithromycin, doxycycline, ofloxacin, and josamycin (Bebear et al. 2000; Sprong et al. 2020; Waites et al. 2020; Yang et al. 2020). Given the serious sequelae and resistance to broad-spectrum antibiotics, the isolation and characterisation of novel immunological targets against Uu to develop an effective vaccine is urgently required. Immunisation is the most effective and economical approach, as premeditated eradication is better than repeated recurrences (Abbas et al. 2020). Although numerous vaccination strategies against Uu are being developed (e.g., Uu-GrpE, Uu-50S ribosomal protein L2, or Uu-IscS), no licensed vaccine is currently available (Shiraganavar and Madagi 2021; Tang et al. 2020).

Inside host immune cells such as macrophages and dendritic cells (DCs), Uu encounters various stressful conditions. Previously, we found that host oxidative stress could be an important aspect of Uu pathogenesis (Dai et al. 2015; Qin and Chen 2019). Therefore, to combat oxidative stress such as heat shock and nutrient deprivation, the invading pathogens usually express a large heat shock protein (HSP) repertoire that helps them survive (Colaco et al. 2013; Zügel and Kaufmann 1999). In recent years, growing evidence has revealed that bacterium-derived HSP70 is essential for DCs maturation and lymphocyte activation and is highly immunogenic during infections (Fang et al. 2014; Matsui et al. 2021). In Uu, the HSP70 system comprises GrpE (Uu0450)-DnaK (Uu0346)-DnaJ (Uu0451), and the genes for these three proteins are expressed together (Bracher and Verghese 2015; Tang et al. 2020). Previously, we found that vaccination with recombinant Uu-GrpE led to a decrease in the pathogen burden and inflammatory responses in the uterine tissues in a BALB/c mouse *U. urealyticum* vaginal-challenge model (Tang et al. 2020). However, Uu-DnaJ, as a candidate vaccine molecule, has received relatively less attention.

In the present study, we aimed to investigate if vaccination with recombinant DnaJ (with Freund's adjuvant) induces antigen-specific antibodies and cell-mediated immune responses to eliminate Uu. In addition, we aimed to assess the effects of DnaJ on BMDCs activation and their subsequent effect on the Th1 cell-biased response, which could tentatively indicate that DnaJ immunisation could induce a Th1 immune cascade-related reaction and, consequently, efficiently protect mice against *U. urealyticum* infection.

Materials and methods

DnaJ protein sequence retrieval

The complete (Uniprot Accession No. B5ZBQ4) amino acid sequence of *U. urealyticum* DnaJ was obtained from UniProt (<http://www.uni-prot.org>) in the FASTA format. DnaJ sequence conservation across different serovars of *U.*

urealyticum was analysed using BLASTp (<http://www.ncbi.nlm.nih.gov/BLAST/>), with a sequence identity of > 95% and a coverage percentage of > 95%.

Analysis of physicochemical properties

Three physicochemical properties of the *U. urealyticum* DnaJ protein were analysed, including the theoretical number of transmembrane helices, molecular weight (MW) and isoelectric point (pI). The MW and pI were determined using ExPasy ProtParam (<https://web.expasy.org/protparam/>). Transmembrane helices were studied using TMHMM (<https://services.healthtech.dtu.dk/service.php?TMHMM-2.0>), with a cut-off < 1.

Structure prediction and assessment

The AlphaFold 2 server (Jumper et al. 2021) was used to predict the DnaJ 3D structure. Validation of the predicted 3D model through the generation of a Ramachandran plot was performed using PdbSum (<http://www.ebi.ac.uk/thornton-srv/databases/pdbsum/Generate.html>).

Antigenic epitope mapping

To determine the B-cell candidate linear epitopes, the full-length DnaJ protein sequence was analysed using BepiPred 2.0 (<https://services.healthtech.dtu.dk/service.php?BepiPred-2.0>), with a 0.55 cut-off and a 15-me epitope length, and using ABCpred (<http://www.imtech.res.in/raghava/abcpred>), with a 0.80 threshold value and a 16-me epitope length. Next, ElliPro (<http://tools.iedb.org/elliopro/>), available in IEDB, was used to perform structural B-cell epitope prediction, with a threshold value of > 0.5, using the 3D model of DnaJ. Finally, the antigenicity of the linear and structural B-cell epitopes was further assessed using Vaxijen V2.0 (<http://www.ddg-pharmfac.net/vaxijen/VaxiJen/VaxiJen.html>).

To predict the cytotoxic T-lymphocyte (CTL) epitopes, we followed the method reported by Grifoni et al. (Grifoni et al. 2020), scoring all peptides with the frequent HLA allele models, selecting the top 1% scoring peptides in the DnaJ sequence. For the helper T-lymphocyte (HTL) epitopes prediction, we applied a previously reported method with modifications (Grifoni et al. 2020; Paul et al. 2015), using the TepiTool resource in IEDB (<http://tools.iedb.org/tepitool>) and a median consensus percentile of < 20, which corresponds to a target-specificity threshold of 50%.

U. urealyticum and culture conditions

The standard strain of *U. urealyticum* serovar 8 (ATCC 27,618) was cultivated in a pleuropneumonia-like organism with 16%

foetal bovine serum (FBS; A3160801, Gibco, USA), 0.3% urea, 0.002% phenol red and 1000 U/mL penicillin G. As described previously (Reyes et al. 2009; Tang et al. 2020), Uu culture dilutions were inoculated onto a solid medium and incubated at 37 °C for 5 days to determine CFUs.

Recombinant DnaJ (rDnaJ) expression and purification

The genomic DNA (gDNA) of *U. urealyticum* strain 8 was used as a template for PCR to amplify the full-length DnaJ gene sequence. The following primers were used: forward primer, 5'-CGGGATCCATGGCGAAACGTGACTACTACG-3' (the *Bam*HI site is underlined); and reverse primer, 5'-CCGCTCGAGTTACTGCATCAAGCGGAGTTATTTGTTTCAC TTCTTTCAGCAGTTT-3' (the *Xho*I site is underlined). The target DnaJ fragment (1,128 bp) was cloned into the expression vector pET28a using the *Bam*HI and *Xho*I restriction sites, which harbour the His6 tag at the N-terminus. Recombinant pET28a-DnaJ was transformed into *E. coli* BL21 (DE3) cells. Before expression, the target DnaJ fragment integrity in the vector was confirmed by double digestion and sequencing.

The rDnaJ expression was induced by 100 µg/mL kanamycin and 0.5 mM isopropyl-β-d-thiogalactosidase (IPTG) at 37 °C for 4 h. Bacterial cells were harvested and re-suspended in lysis buffer (10 mM imidazole, 20 mM NaH₂PO₄, 50 mM Tris-HCl (pH 7.8), 300 mM NaCl, 20% glycerol, and 1% Triton X-100). For easy purification, rDnaJ with a His6 tag was expressed as a soluble protein, purified by Ni-NTA affinity chromatography, and step-eluted with different concentrations of imidazole (100–300 mM). The purified recombinant protein was investigated by 12.5% sulphate polyacrylamide gel electrophoresis (SDS-PAGE). Once purified, rDnaJ was treated with ToxinEraser™ Endotoxin Removal Kit (L00338, GenScript, Piscataway, NJ). Endotoxin levels were measured by the Limulus assay test (2,107,212, Zhanjiang Bokang Marine Biological Co., China) and did not achieve significant levels.

Mice

Studies were performed on 4–6-week-old female BALB/c mice and C57BL/6 mice from the Hunan SJA Laboratory Animal Co., China (Approval No. SCXK-Hunan-2019–0004). Specific-pathogen-free mice were housed in a barrier facility and handled by authorised personnel. All protocols were approved by the Institutional Animal Use Committee of the University of South China (approval number USC202009XS07).

BMDCs generation and stimulation

BMDCs were generated from C57BL/6 bone marrow precursors according to a previously described procedure

(Inaba et al. 1992; Kim et al. 2018). Briefly, the bone marrow precursors were differentiated for 6 d in Roswell Park Memorial Institute (RPMI)-1640 with 15% FBS, 10 ng/mL granulocyte–macrophage colony-stimulating factor (Hangzhou Kaihua Biotechnology Co., China), 10 ng/mL IL-4 (214–14-20, PeproTech, USA) and 100 U/mL penicillin/streptomycin at 37 °C with 5% CO₂. Flow cytometric analysis confirmed the isolated cell purity (Figure S1). Immature BMDCs (5 × 10⁶ cells/well) were plated onto 24-well plates and pulsed with DnaJ.

Cytotoxic assay

The BMDCs in the 24-well plates were incubated with DnaJ (5–80 µg/mL) for 48 h. The culture supernatant was collected and cytotoxic effects were determined using the Lactate dehydrogenase (LDH) assay kit (A020-1, Nanjing Jiancheng Bioengineering Institute, Nanjing, China). The protocol has been described in a previous report (Geng et al. 2020; Liu et al. 2020). In brief, LDH leakage was determined using the following equation: [(sample OD_{440nm} value) – (negative control OD_{440nm} value)] / [(positive control OD_{440nm} value) – (negative control OD_{440nm} value)] × 2 × 1000. LDH leakage (U/L) was expressed as the percent of total LDH activity that was present in the supernatant.

Immunisation protocols

Purified recombinant protein Uu-DnaJ (50 µg), emulsified with 100 µL of Freund's complete adjuvant (Sigma-Aldrich, St. Louis, MO, USA) for the first inoculation (injected intramuscularly; 0 weeks), followed by two booster inoculations at 2-week intervals with Freund's incomplete adjuvant (2 and 4 weeks). Negative control mice were injected with equal amounts of PBS or FA (PBS was emulsified in Freund's adjuvant) at the immunising site. Serum samples were collected from the tail vein of each mouse weekly (0, 1, 2, 3, 4, 5, and 6 weeks). Two weeks after the last immunisation, the mice were euthanised and splenocytes were isolated for the immunoassays.

Genital tract infection challenge

Groups of mice were challenged with 1 × 10⁷ CFU *U. urealyticum* (re-suspended in 30 µL of PBS) intravaginally 2 weeks after the last immunisation. Prior to the challenge, the oestrus cycle was synchronised by neck subcutaneous treatment with oestradiol benzoate (0.5 mg/mouse), increasing susceptibility to *U. urealyticum* infection. On days 7 and 14 after the genital challenge, vaginal secretions were collected using *U. urealyticum* liquid medium (1 mL) and swabs, and mice were euthanized. For upper genital tract secretions collections, the uterus was cut open

longitudinally, and each uterine horn and cervix were flushed with 1 mL of liquid medium. The samples were serially diluted with *U. urealyticum* liquid medium at multiple ratios. For CFU determination (Reyes et al. 2009), 100 µL from each sample and its corresponding dilutions were plated on *U. urealyticum* solid medium (0.9% agar). The number of colonies was counted in at least six randomly selected fields under an optical microscope (Noh et al. 2019).

Western blot analysis

Three microliters of DnaJ lysate was separated by SDS-PAGE in a 12.5% gel and blotted onto a previously rehydrated polyvinylidene fluoride membrane. After 3 h of blocking with 5% skimmed milk and washing twice with Tris-buffered saline with Tween-20 (TBST), the membrane with the protein was incubated with DnaJ-immunised mouse serum or (Uu-serum) as the primary antibody and then kept overnight at 4 °C on a shaker. The following day, after four washes with TBST, the bands were incubated with anti-mouse IgG antibodies conjugated with horseradish peroxidase (HRP; 1:5000) (7076P2, Cell Signaling Technology, MA, USA) for 1.5 h at 37 °C. After the blots were rewashed with TBST, they were exposed to a chemiluminescence instrument (CLINX-6300, China). Finally, images were obtained using a film developer (EPSON-V370, Japan).

ELISA

The antigen-specific antibody responses were assayed using ELISA in 96-well plates. For the antibody titres, the plates were coated with purified rDnaJ (10 µg/mL, 100 µL/well) overnight at 4 °C. The microplates were then blocked with 5% skim milk at 37 °C for 2 h. After blocking, the microplates were washed four times with PBS containing Tween 20 (PBST). The serum samples were serially diluted from 1:100 to 1:204,800 in dilution buffer, and 100 µL of the diluted serum was added to each well. After 2 h of incubation at 37 °C, the microplates were washed six times with PBST and HRP-conjugated goat anti-mouse IgG (1:10,000) was distributed into each well for 1 h at 37 °C. Then, 3,3',5,5'-tetramethylbenzidine (substrate (100 µL/well) was added, the microplates were incubated at 37 °C for 20 min and the reaction was stopped using 2 N H₂SO₄. The absorbance of the plates was measured at 450 nm using a microplate reader (Multiskan Mk-3, Thermo Fisher Scientific). The antibody titres were determined as the highest dilution of serum giving a detectable absorbance reading 2.1 times above the background average. To measure the serum IgG, IgM, IgG1, IgG2a, IgG2b, and IgG3 responses, the microplates were coated with DnaJ. On the following day, the plates were incubated with the serum samples from the mice (1: 100 diluted in 5% non-fat milk in PBST).

Horseradish peroxidase-conjugated goat anti-mouse IgM, IgG1, IgG2a, IgG2b, or IgG3 (SA00012-6, SA00012-1, SA00012-2, SA00012-3, SA00012-5, ProteinTech Group, USA) was added at a 1:1,000 dilution to the designated well, following the same procedure as above. To characterize the serum *U. urealyticum*-specific IgG response, 300 µl of 25% glutaraldehyde was loaded to each well of a 96-well high-binding microtiter plate (Corning Incorporated), incubated for 2 h at 37 °C, and washed three times by deionized water. The 96-well plate (Corning Incorporated) was coated with 100 µl/well of 5 × 10⁶ CFU *U. urealyticum*. Plate was then incubated with pooled sera from PBS-, FA- and DnaJ-vaccinated mice (1:100), and anti-Uu antibodies were detected using an HRP-conjugated anti-mouse IgG.

Cytokine quantification

Cytokine levels were determined in mouse splenocytes and BMDCs. The splenocytes were cultured at 2 × 10⁶ cells/well in 24-well plates and stimulated with DnaJ (10 µg/mL) for 48 h. Alternatively, BMDCs (5 × 10⁶ cells/well) were treated with 5–20 µg/mL DnaJ for 24 h. Then, supernatants were collected to measure the levels of secreted cytokines such as IFN-γ, TNF-α, IL-4, IL-10, IL-1β, IL-6, and IL-12p70 using the corresponding mouse ELISA kits, according to the manufacturer's instructions (88-7314-22, 88-7324-22, 88-7044-22, 88-7105-22, 88-7013-22, 88-7064-22, eBioscience, USA).

Flow cytometry analysis

Mouse BMDCs or splenocytes were washed with PBS. For surface marker extracellular staining, the cells were incubated with anti-mouse CD11c (557,400, BD Biosciences), CD80 (560,526, BD Biosciences), CD86 (552,692, BD Biosciences), MHC-II (562,367, BD Biosciences), CD11b (101,211, Biolegend), CD4 (553,046, BD Biosciences), or CD8 antibodies (551,162, BD Biosciences) at 4 °C for 30 min. For intracellular cytokine staining, the splenocytes were stimulated with DnaJ (10 µg/ml) for 8 h in presence of Golgi plug™ (51-2301KZ, BD Bioscience). The splenocytes were then treated for surface markers (CD4 or CD8), fixed/permeabilised with a Cytofix/Cytoperm solution (51-2090KZ, BD Bioscience) and then stained with anti-IFN-γ (557,735, BD Biosciences) and anti-IL-4 (554,435, BD Biosciences) antibodies at 20–25 °C for 30 min. All events were acquired on a FACSverse flow cytometer and analysed using the FlowJoV software (Tree Star).

To determine cytokine (IFN-γ, TNF-α, IL-1β, IL-10, IL-17a, MCP-1, IL-1α, and IL-6) concentrations in the uterine tissue, multi-analyte flow assay kits (740,446, Biolegend, San Diego, CA, USA) were used as indicated by the manufacturer.

Histopathology

The mice were immunised with DnaJ and challenged with *U. urealyticum*, as described above. The reproductive tract was removed from immunised mice 14 days after infection, fixed with 4% paraformaldehyde, and embedded in paraffin, and the paraffin-embedded reproductive tract samples (including the uterine horn) were cut into sections. For histological evaluation, the tissue sections were stained with haematoxylin and eosin (H&E). All tissue sections were blindly evaluated by two pathologists.

Detection of endotoxin removal effect in DnaJ

The endotoxin removal effect in the rDnaJ detection method was modified from a previous study (Kim et al. 2018). DnaJ was incubated in PBS containing 10 µg/mL PMB (polymyxin B) for 3 h at 4 °C. Moreover, for heat-inactivation (Boiling), DnaJ was incubated at 100 °C for 2 h. After 24 h of antigen pulsing, the surface molecules (CD80, CD86, and MHC-II) expression levels in CD11c⁺ BMDCs were measured by flow cytometry analysis.

BMDCs and naïve T-cell co-culture

The allogeneic T cells were isolated from BALB/c mouse splenocytes using MojoSort™ Mouse Naïve CD4 T cell Isolation Kit (480,040, BioLegend, USA) and co-cultured with BMDCs at a ratio of 1:10 for 4 days. The levels of IFN-γ, IL-4, IL-5, and IL-10 were quantified on the culture supernatant using commercially available ELISA kits.

Adoptive immunisation with DnaJ-pulsed BMDCs

The BMDCs were cultured and stimulated as described above. Six-week-old female C57BL/6 mice (four per group) were immunised with intravenous injection of 2×10^6 mature DnaJ-pulsed BMDCs (0 day). Booster immunisation was performed with the same number of DnaJ-pulsed BMDCs (7 days). Each mouse received a total of two immunizations. Control groups were injected with equal amounts of PBS or untreated BMDCs. Serum was collected from all mice and these were sacrificed to isolate splenocytes for subsequent experiments (ELISA or flow cytometry analysis).

Statistical analyses

Statistical analysis was performed using one-way ANOVA followed by the Duncan test. All results are expressed as mean ± standard error of the mean. Prism version 8 software (GraphPad Inc, San Diego, CA, USA) was used for analysis. *P* values lower than 0.05 were considered significant (*, $P < 0.05$; **, $P < 0.01$; ***, $P < 0.001$; ****, $P < 0.0001$).

Results

DnaJ is conserved among the *U. urealyticum* serovars

The BLASTp analysis results indicated that the DnaJ protein sequence revealed a high sequence conservation degree (sequence similarity > 99%) among the different *U. urealyticum* serovars, thus acting as an effective target for broad-spectrum vaccine development (Table S1).

Physicochemical property assessment

The Uu-DnaJ protein contains 375 amino acids with a MW of approximately 41.79 kDa and a theoretical pI of 8.04. Previous studies have shown that proteins with low MW (< 110 kDa) are regarded as attractive vaccine targets, as they can be easily purified (Abbas et al. 2020). In addition, transmembrane helix analysis revealed that DnaJ is a preferred target, as it has no transmembrane helix and can therefore be easily cloned and expressed.

Protein structure modelling and validation

The DnaJ 3D structure was subjected to the PdbSum server to assess the Ramachandran plot statistics. The plot showed that 91.2% of the residues were present in the most favoured core regions (yellow colour), 7.6% in the additionally allowed region (yellow colour), 0.9% in the generously allowed region (pale yellow colour), and 0.3% in the disallowed regions (white colour) (Fig. 1A). The results showed that the model structure had good quality and high stability. Moreover, The full DnaJ protein 3D structure model is shown in Fig. 1B. The key to successful predictive identification of DnaJ epitopes is the visualization of their 3D structure.

B-cell epitope prediction and evaluation

The B-cell linear epitope in DnaJ was predicted using Immune Epitope Database (IEDB) and the BepiPred 2.0. The results showed that BepiPred 2.0 predicted seven epitopes, whereas ABCpred predicted eight epitopes. ElliPro predicted six discontinuous B-cell epitopes in the DnaJ 3D structure (Fig. 1C). Interestingly, all the predicted linear and structural B-cell epitopes maintained their VaxiJen scores of > 0.4.

T-cell epitope prediction and assessment

The CTL epitopes were predicted using the NetMHCpan 4.0 EL algorithm available at IEDB, using the method described by Grifoni et al. (Grifoni et al. 2020). Based on the final ranking scores (1% scoring peptides), we obtained eight CTL epitopes (Table S2). In parallel, following a previously

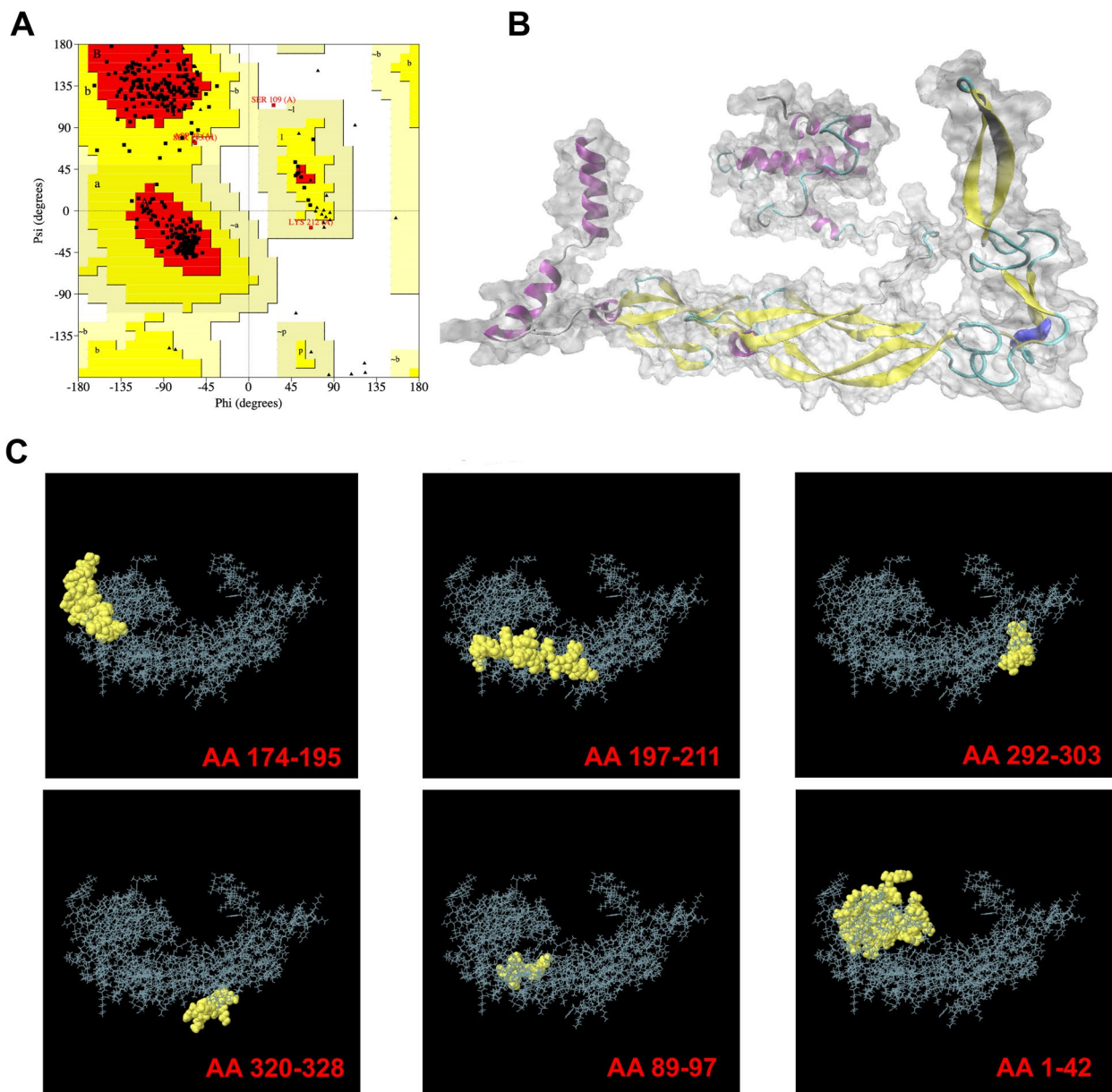


Fig. 1 Bioinformatics analysis of DnaJ based on the amino acid sequences. **A** Ramachandran plots. **B** Three-dimensional (3D) structure of DnaJ. **C** Conformational B-cell epitopes of DnaJ. AA₁₇₄₋₁₉₅: TIENVHSLFGTIQQEVECHECE; AA₁₉₇₋₂₂₁: TGKVANSKCEQ-

CYGKKVINERNVLT; AA₂₉₂₋₃₀₃: SGIKTIEIPPNT; AA₃₂₀₋₃₂₈: KPNIFSKKN; AA₈₉₋₉₇: GGVDVDIND, AA₁₋₄₂: MAKRDYYEVLGVSKSASPEEIKTAFRKLAKHEHPDRNKSADD; AA: amino acid position

reported approach (Grifoni et al. 2020; Paul et al. 2015), we used the Tepitool resource in IEDB and identified seven HTL epitopes in the DnaJ sequence (Table S3).

rDnaJ expression and purification

As shown in Fig. 2A, the plasmid pET28a/DnaJ was successfully constructed and transformed into *E. coli* BL21 (DE3). DnaJ was successfully expressed in *E. coli*

following the induction with IPTG (0.5 mM). The SDS-PAGE results revealed a protein of ~41.79 kDa MW (Fig. 2B). rDnaJ was purified by nickel-nitrilotriacetic acid (Ni-NTA) affinity chromatography and the purity was more than 90% (Fig. 2C). Subsequently, protein purification was confirmed by western blot analysis using Anti-His (Fig. 2D, Lane 13). Also, we show that Anti-*U. urealyticum*-infected mouse serum (Uu-serum) recognized rDnaJ (Fig. 2D, Lane 14–15).

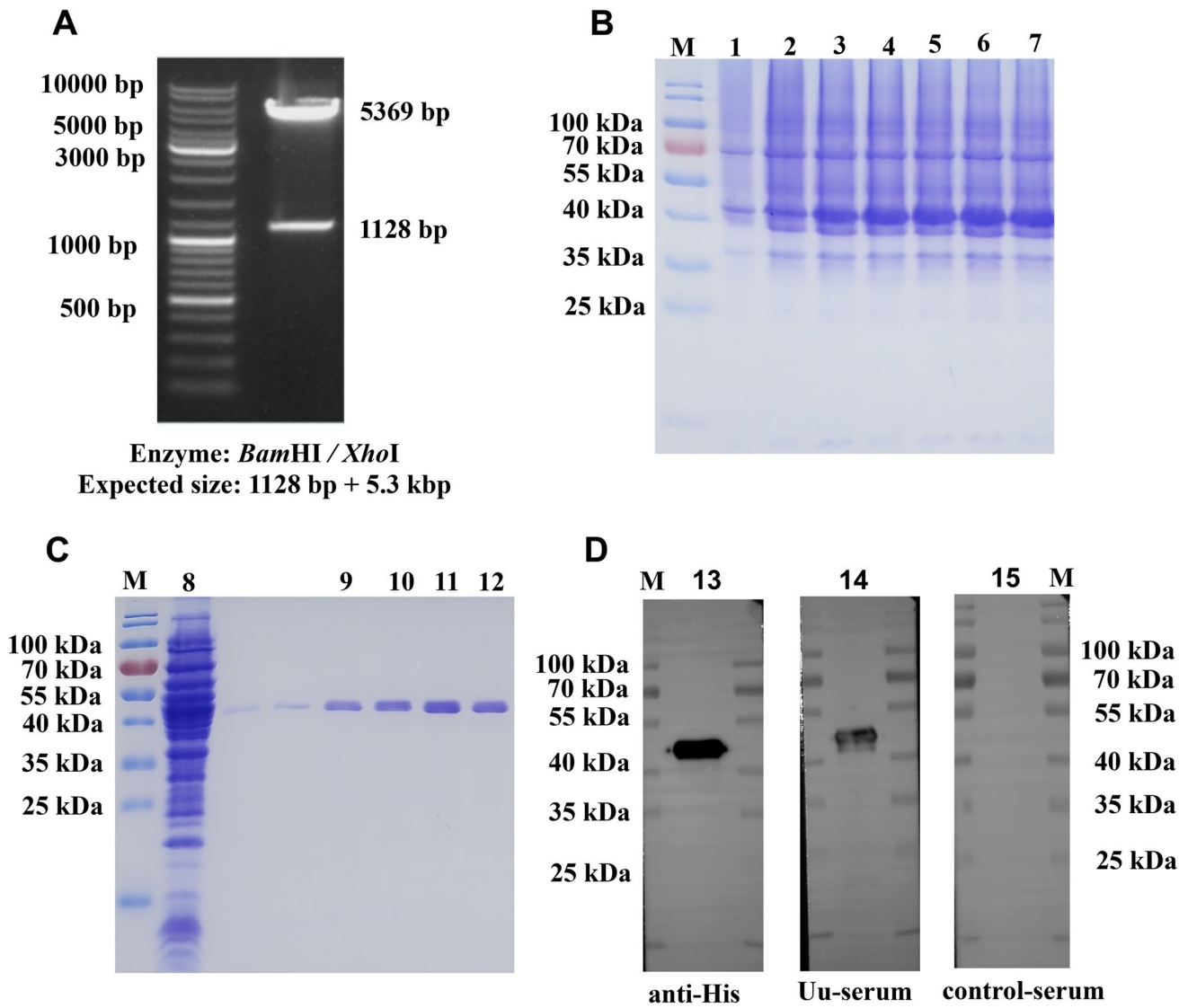


Fig. 2 Enzyme digestion results. **A** Polymerase chain reaction successfully amplified the expected DnaJ gene band (1128 bp) and the DnaJ gene in *E. coli* BL21(DE3) was cloned using the pET28a vector and *Bam*HI and *Xho*I restriction sites. Preparation of the recombinant DnaJ protein: **B** Under optimum inducement conditions, DnaJ was over-expressed in *E. coli* BL21(DE3) (lanes 3–7; compare lanes 1

and 2, Under non-optimum inducement conditions). **C** 12.5% sodium dodecyl sulphate -polyacrylamide gel electrophoresis analysis of the DnaJ protein purification (lanes 8, uninduced; lanes 9–12, DnaJ was purified by using eluates of 100, 150, 200, and 250 mM of imidazole). **D** Western blot analysis of the DnaJ protein using anti-His, Uu-serum and control serum (lanes 13–15)

DnaJ immunisation induced DnaJ-specific antibody and cell-mediated immunity responses in mice

To determine the role of DnaJ in humoral immune response, DnaJ-specific antibody levels in the mouse serum were measured. Compared with those of the phosphate-buffered saline (PBS) and Freund’s adjuvant (FA) groups, the DnaJ-immunised mice generated considerable immunoglobulin G (IgG) antibody titres over time (Fig. 3A). To further characterise IgG isotype distribution (IgG1, IgG2a, and IgG3) present in the serum, we performed an enzyme-linked immunosorbent assay (ELISA) to determine these antibody

levels. A significant amount of serum IgG subclass antibodies was detected in the DnaJ-vaccinated mice. The serum IgG subclass antibody levels induced in the recombinant antigen DnaJ group were also higher than those in the FA and PBS groups. The responses were indicative of the Th1 response to IgG2a and IgG3 antibodies that were as easy to detect as IgG1 antibodies. In addition, asynchronous IgM and IgG seroconversion was observed after DnaJ vaccination (Fig. 3B). We also observed that DnaJ-immunised mouse serum but not control mouse serum recognised the purified DnaJ protein by western blot analysis (Fig. 3C). To characterize whether sera from DnaJ vaccinated mice could

recognize Uu, we performed ELISA experiments with *U. urealyticum* serovar 8. The data obtained indicate that the serum from DnaJ-vaccinated mice can bind to intact bacteria (*U. urealyticum*) above the background threshold (Fig. 3D).

Previous studies have demonstrated that Th1 immune responses reduce the severity of metritis caused by *U. urealyticum*. To explore the type of cell-mediated immunity responses elicited by DnaJ immunisation, we first identified the cytokine levels in the splenocyte culture supernatants after stimulation during ELISA. Classical TNF- α and IFN- γ (Th1 cytokines) secretion was increased in DnaJ-immunised animals (Fig. 4A), whereas IL-4 and IL-10 (Th2 cytokines) levels were nearly undetectable. We also observed a significant increase in the IFN- γ ⁺ CD4⁺ T and IFN- γ ⁺ CD8⁺ T cell percentages in DnaJ-immunised mouse splenocytes (Fig. 4B). Conversely, we did not observe such a difference in the IL-4⁺ CD4⁺ T cell

percentage. These results suggested that DnaJ vaccination leads to a Th1 polarisation response.

DnaJ immunisation reduces the bacterial burden and inflammatory response in the uterus caused by *U. urealyticum*

The ability to confer protection against infection is a critical feature of a valid *U. urealyticum* vaccine. As described above, the mice were vaccinated with DnaJ and infected with *U. urealyticum* (1×10^7 colony-forming units (CFUs)/30 μ L). Vaginal and upper genital tract secretions were collected on the indicated days after the challenge. The positive Uu culture in secretions to be demonstrated the successful infection. On day 14 post-infection, we observed that all mice exhibited increased vaginal secretions, hair loss, vaginal redness, and swelling, but the DnaJ-immunised group had relatively

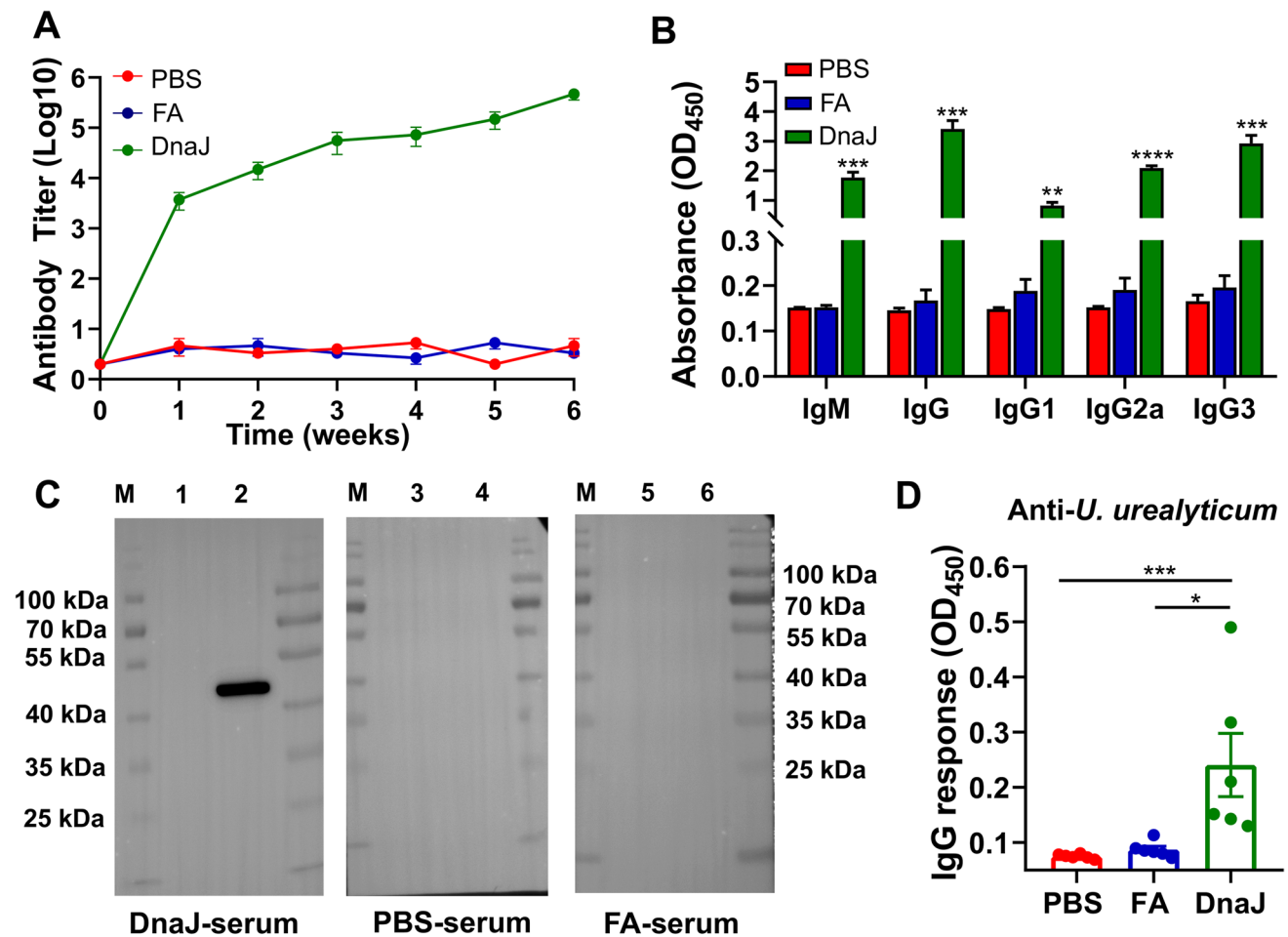


Fig. 3 Detection of the DnaJ-specific antibodies in immunised mice. **A** Anti-DnaJ IgG antibody titres ($n=4$ mice per group). **B** Elicited IgM and IgG subclass (IgG1, IgG2a, and IgG3) in vaccinated mice ($n=4$ mice per group). $**P<0.01$, $***P<0.001$, and $****P<0.0001$. **C** Western blot analysis of purified DnaJ (C, Lane

2, 4 and 6) and the lysate of bacteria transformed with the empty pET28a plasmid (C, Lane 1, 3 and 5) using DnaJ-immunised mouse serum, phosphate-buffered saline (PBS)- and Freund's adjuvant (FA)-mouse serum. **D** IgG response of sera from PBS, FA, and DnaJ vaccinated mice using *U. urealyticum* serovar 8 as antigen

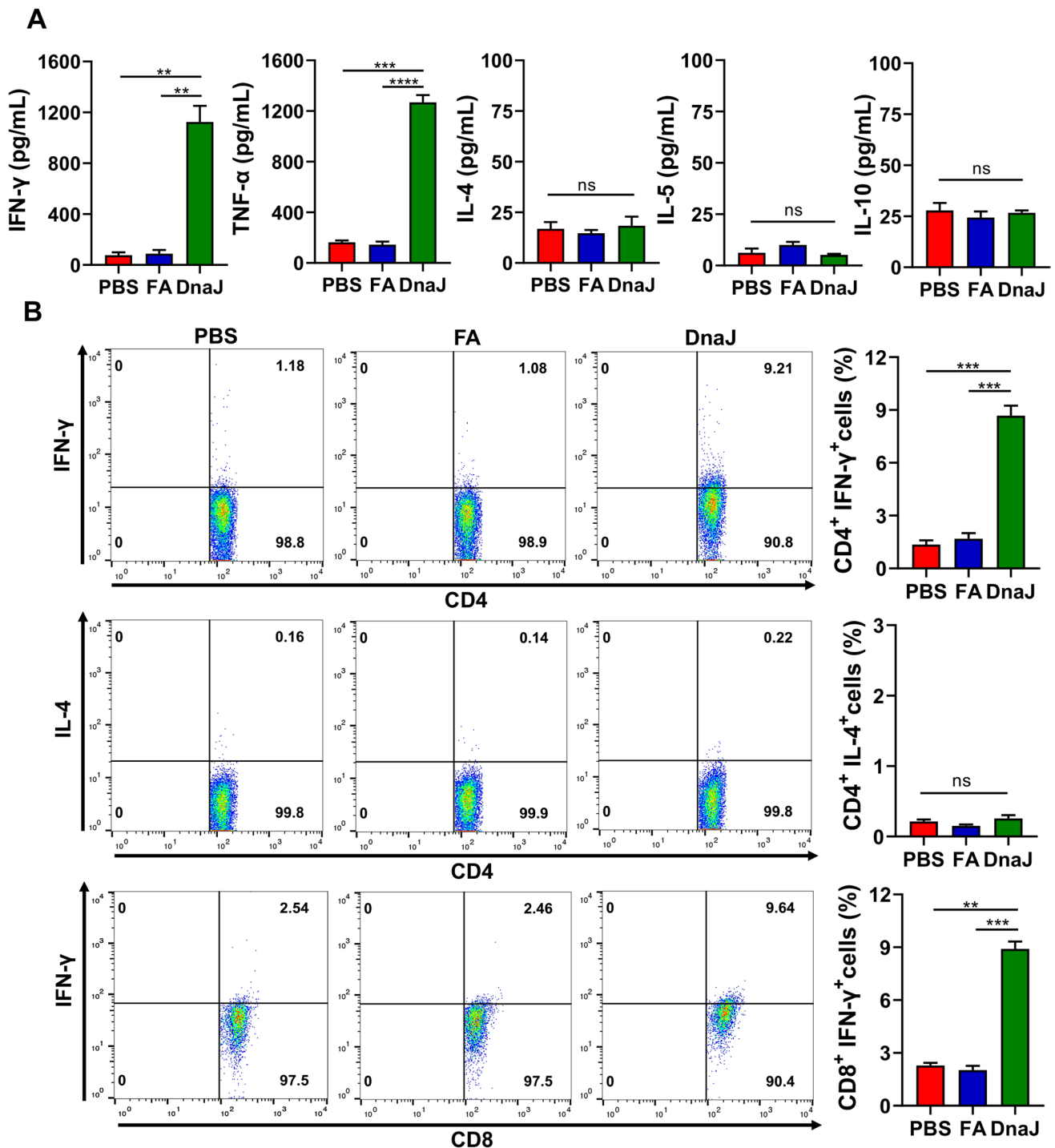


Fig. 4 The DnaJ vaccine with FA predominantly induces Th1-cytokine production in mice. **A** The splenocytes were isolated from PBS -, FA-, and DnaJ-vaccinated groups and stimulated with 10 μg of DnaJ for 48 h in vitro. The levels of IFN-γ, TNF-α, IL-4, and IL-10 in the cell supernatants were measured by enzyme-linked immunosorbent assay ($n=4$ mice per group). ** $P < 0.01$, *** $P < 0.001$,

**** $P < 0.0001$, and ns=not significant, $P > 0.05$. **B** The DnaJ vaccine with FA induced the generation of IFN-γ-secreting CD4⁺ and CD8⁺ cells: Proportion of IFN-γ⁺ CD4⁺ cells in the splenocytes. The proportion of IL-4⁺ CD4⁺ cells in the splenocytes. The proportion of IFN-γ⁺ CD8⁺ cells in the splenocytes. ** $P < 0.01$, *** $P < 0.001$, and ns=not significant, $P > 0.05$

mild symptoms (Figure S2). Bacterial burden in the vaginal and upper genital tract secretions was determined at both 7 and 14 days post-challenge. As expected, immunisation with

rDnaJ resulted in decreased *U. urealyticum* load in the genital tract secretions in the DnaJ-immunised mouse groups than in the control groups (Fig. 5, PBS or FA groups, $P < 0.05$).

To further understand how DnaJ immunisation mediates protection against Uu, we examined cytokine levels in the uterine tissue. IFN- γ , TNF- α , MCP-1, and IL-1 β levels in the DnaJ-immunised mouse uterine tissue homogenate supernatants were reduced compared with those in the control supernatants (PBS or FA groups, $P < 0.05$; Fig. 6). Nevertheless, no difference in IL-1 α , IL-17a, IL-6, and IL-10 levels was observed between the groups. Overall, DnaJ immunisation significantly lowered the uterus bacterial burden and inflammatory response during *U. urealyticum* challenge.

Protection against uterus pathological changes with DnaJ immunisation

U. urealyticum causes metritis associated with acute inflammation, oedema, and increased production of secretions. To further understand the protective effect of DnaJ, the mice were immunised, and at day 14 post-*U. urealyticum* infection, the uterus was compared for pathological changes in all groups of mice. The DnaJ-immunised mice had a lower inflammatory cell (such as polymorphonuclear leukocytes) recruitment than that of the control group (Fig. 7). Additionally, the uterine tissue sections from the PBS and FA groups showed severe pathological features such as epithelial shedding/necrosis within the uterine lumen, increased glandular secretions and dilated glandular ducts. Conversely, DnaJ-immunised mice showed uterine tissues with an intact endometrial layer with tubular structures and a clear small lumen.

DnaJ induces BMDCs activation

DCs, professional antigen-presenting cells (APCs), are of particular interest during vaccination. To further determine whether *U. urealyticum* DnaJ induces DCs activation, we first examined inflammatory cytokine secretion by DnaJ-stimulated BMDCs in cultured supernatants. DnaJ exhibited a dramatic increase in IL-1 β , IL-6, IL-12p70, and TNF- α

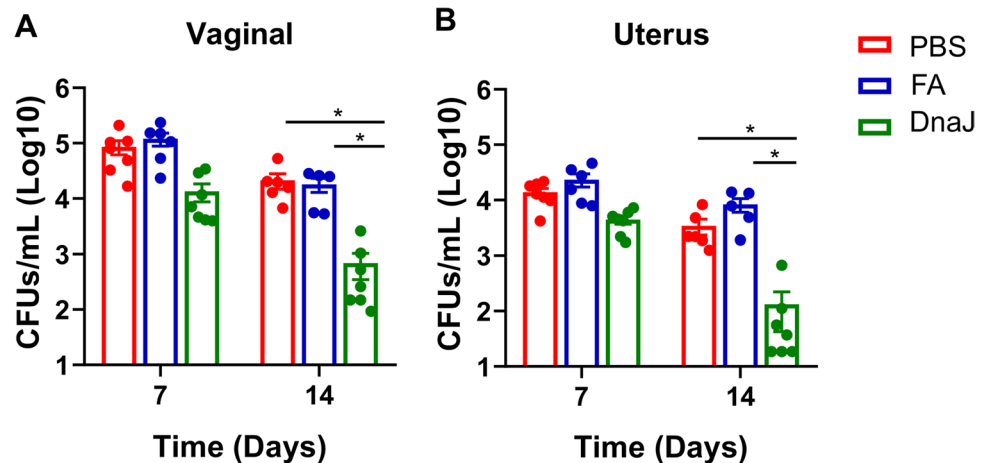
production in a dose-dependent manner (Fig. 8A). Additionally, we analysed surface molecule expression in BMDCs. DnaJ significantly increased surface molecule (CD80 and CD86) and MHC class II expression in BMDCs (Fig. 8B). Therefore, DnaJ directly induced BMDCs activation and maturation. Next, to investigate the possible contributions of trace amounts of residual lipopolysaccharide, DnaJ was subjected to PMB treatment or inactivated by heat. PMB pretreatment did not affect the DnaJ ability to trigger BMDCs activation. However, heat inactivation significantly inhibited DnaJ (Fig. 8B, compared with untreated DnaJ, $P < 0.05$). Additionally, we found no remarkable differences in the cytosolic marker lactate dehydrogenase (LDH) release upon DnaJ stimulation (Figure S3). In summary, DnaJ induced BMDCs maturation independent of cell damage or contaminating endotoxins.

DnaJ-pulsed BMDCs promote CD4 Th1 immune responses

Th1 cell cytokines, especially IFN- γ , are critical for *U. urealyticum* clearance. To examine whether DnaJ-pulsed BMDCs induced the CD4 naïve T cells towards an IFN- γ -producing Th1 cell phenotype, ELISA was performed to examine Th1/Th2 cytokine expression in the BMDC-naïve T cell co-culture system. DnaJ-pulsed BMDCs significantly increased IFN- γ secretion by T cells (Fig. 9A, compared with the DnaJ-BMDCs or BMDCs-T cell groups, $P < 0.01$). In contrast, IL-4, IL-5, and IL-10 were not induced.

Finally, we vaccinated naïve mice with DnaJ-pulsed BMDCs, PBS-pulsed BMDCs, or PBS (intravenous injection). As expected, the DnaJ-specific Th1 cells (IFN- γ^+ CD4 $^+$) were detected in the adoptive immunisation of mice with DnaJ-pulsed BMDCs (Fig. 9B). However, we did not observe a significant difference in the percentage of Th2 cells (IL-4 $^+$ CD4 $^+$) in the splenocytes of DnaJ-pulsed BMDCs group compared with that of the PBS-pulsed BMDCs or PBS groups. Next, we

Fig. 5 DnaJ-immunisation reduced *U. urealyticum* load in the reproductive tract of infected mice. The burden of *U. urealyticum* in reproductive tract secretions was quantified by bacterial culture ($n = 5-7$ mice per group). * $P < 0.05$. **A** Bacterial burden was determined by vaginal CFU count/mL. **B** Bacterial burden was determined by uterus CFU count/mL. Dots represent individual mice



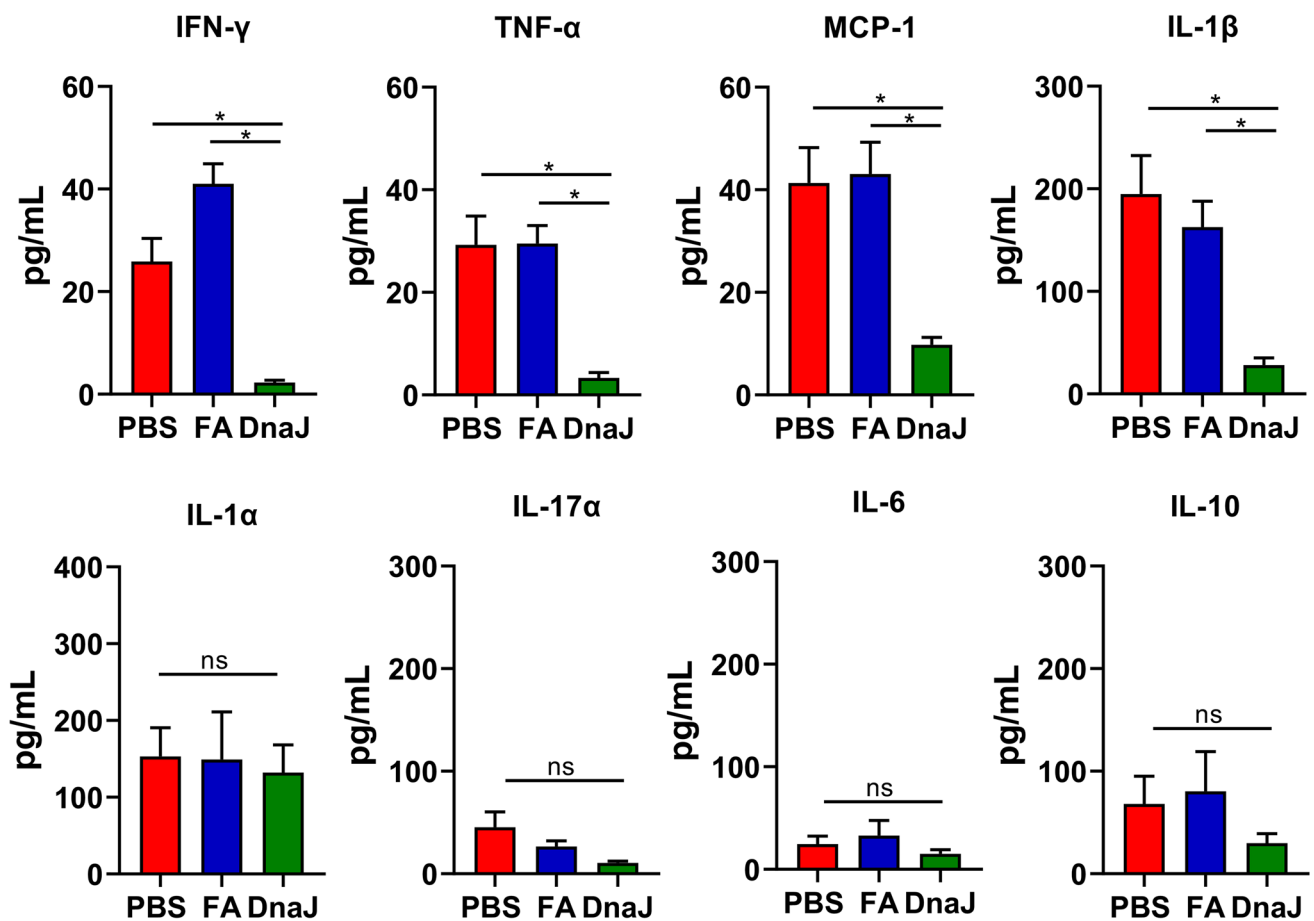


Fig. 6 Cytokine concentrations in the uterine tissue of *U. urealyticum*-infected mice. Concentrations of IFN- γ , TNF- α , MCP-1, IL-1 β , IL-1 α , IL-17 α , IL-6, and IL-10 in the supernatant of the uterine tissue homogenates from the mice after *U. urealyticum* infection, as deter-

mined using a multi-analyte flow assay kit. The cytokine concentrations (pg/mL) in the uterine tissue homogenate ($n=3-6$ mice per group). * $P < 0.05$, and ns = not significant, $P > 0.05$

assessed the serum anti-DnaJ IgG1, IgG2a, IgG2b, and IgG3 antibodies by ELISA and found that mice immunised with DnaJ-pulsed BMDCs showed a Th1-biased IgG2 antibody response. As shown in Fig. 9C, although DnaJ-pulsed BMDC elicited a combination of IgG1, IgG2a, IgG2b, and IgG3 antibodies, it induced higher levels of IgG2a and IgG2b than IgG1. Importantly, the IgG2/IgG1 antibody ratio was significantly higher in the DnaJ-pulsed BMDCs group than in the PBS-pulsed BMDCs or PBS groups (Fig. 9C, right panel, $P < 0.05$). Together, these results established that the use of DnaJ-pulsed BMDCs in vitro induces a Th1 immune response in vivo.

Discussion

Currently, no licenced vaccines against *U. urealyticum* are available (Sweeney et al. 2017; Tang et al. 2020). Here, we showed that rDnaJ vaccination provided protection against *U. urealyticum* challenge. We also attempted to illustrate the increase in the

robust Th1 immune reaction of Uu-DnaJ by showing that DnaJ interacts with DCs and improves vaccine development.

An effective vaccine immunogen should meet the following requirements: (1) it should be highly conserved among *U. urealyticum* serovars; (2) it should be expressed and antigenic during infection and (3) it should elicit long-term protective immunity in vivo (Eslamizar et al. 2021; Li et al. 2018). We observed that Uu-infected mouse serum recognized rDnaJ. Thus, DnaJ was up-regulated during Uu infection suggesting that it is a potential antigen target (Kim et al. 2018; Tang et al. 2020). The protein was expressed in *E. coli* BL21 (DE3). However, other biological impurities from the rDnaJ challenge may be used to develop safe vaccines (Akache et al. 2021; Sen-Kilic et al. 2019). In our study, rDnaJ was purified using Ni-affinity chromatography, and the DnaJ-immunised mouse serum did not recognise bacterial lysates converted to empty pET28a plasmids (see Fig. 3C). Therefore, rDnaJ of *U. urealyticum*-induced immune response can be attributed to itself.

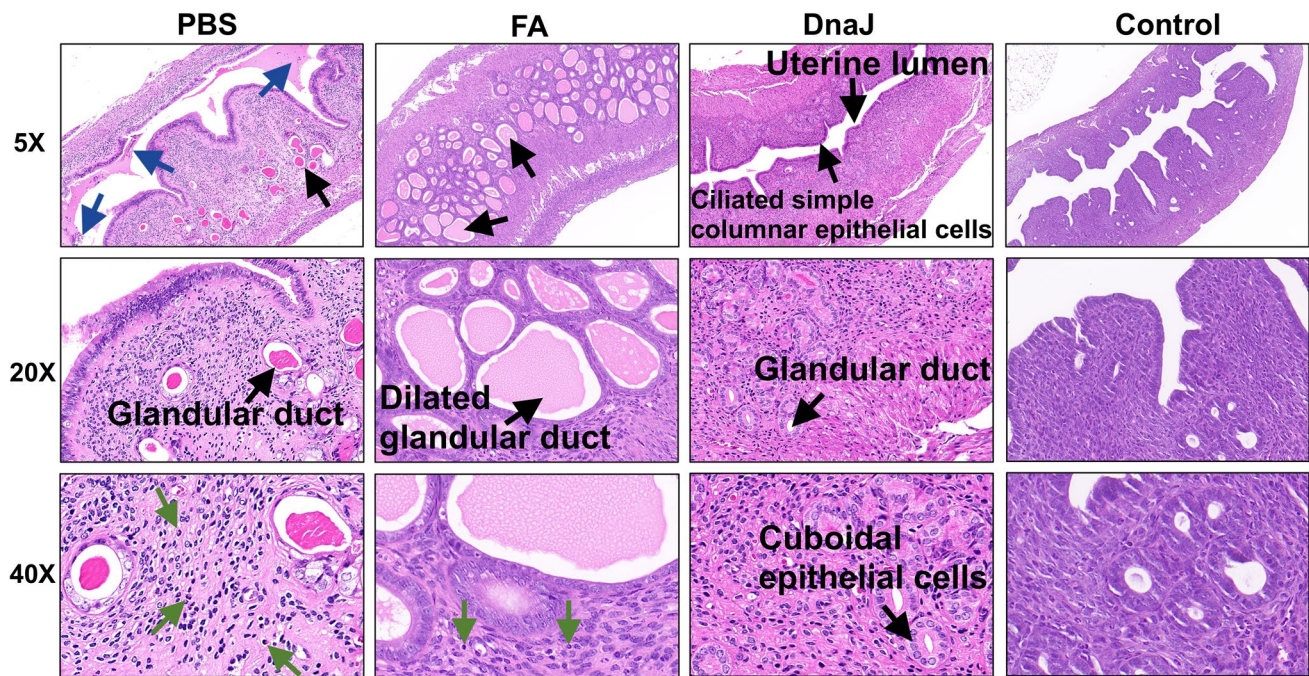


Fig. 7 Pathological lesions of the infected uterine tissues. Haematoxylin and eosin staining in the uterine tissue of each group. The black arrows denote uterine lumen, endometrial layer, or glandular duct.

The blue arrows denote regions of epithelial shedding/necrosis within the uterine lumen. The green arrows indicate inflammatory cells or necrotic cell debris

Some scholars have pointed out that recombinant protein subunit vaccines have limited intrinsic adjuvanticity and require immunogen formulation with adjuvants (Brunham and Rappuoli 2013; Farris et al. 2010; Pal et al. 2020). Previous reports indicated a key role of Th1 cells and neutralising antibodies in protection against pathogen challenge (Li et al. 2019; Ye et al. 2017; Zhao et al. 2016). Therefore, we used a vaccine formulated with DnaJ and Th1 adjuvants (Freund's adjuvant) to elicit protection against genital *U. urealyticum* infection in mice. As expected, the humoral immune responses increased over time in the DnaJ-immunised group and induced strong antigen-specific cellular immunity responses (TNF- α and IFN- γ secretion dominant). It is noteworthy that the DnaJ-vaccinated mice developed specific IgM titers, which progressed to IgG titers, within 21 days after inoculation, and the DnaJ-specific IgG was able to recognize *U. urealyticum* strain. Interestingly, Sen-Kilic et al. showed that a very poorly immunogenic peptide does not result in significant isotype conversion to IgG despite the fact that it can trigger low specific IgM antibody titers (Sen-Kilic et al. 2019). Overall, we do have reason to believe that rDnaJ could be a vaccine candidate. Importantly, the DnaJ-specific immune response demonstrated effective protection—mice immunised with DnaJ (adjuvanted by Freund's adjuvant) and challenged 14 days after boosting exhibited a reduction in *U. urealyticum* load. Furthermore, the Th1 vaccination protocol has a pronounced effect on controlling the extent

of inflammation and protects infected mice against uterine tissue pathology. Colonisation by *U. urealyticum* is related to increased levels of certain pro-inflammatory or inflammatory factors in the uterus (Tang et al. 2020; Viscardi et al. 2002). We observed that many TNF- α and IFN- γ -producing cells appeared in mice after immunisation with DnaJ. Despite this, low levels of inflammatory factors (including TNF- α and IFN- γ) were detected in the uterine tissue upon *U. urealyticum* infection. This may imply that the hallmark Th1 cytokines (IFN- γ and TNF- α) activate innate immune cells such as macrophages and DCs in the uterus for pathogen clearance (Back et al. 2020; Bollyky et al. 2010; Noya et al. 2017). Naturally, Th1 cytokine-activated DCs are also required for the optimal initiation of the host protective Th1 response (Gold et al. 2008). However, our study has limitations, such as the interaction between innate and adaptive immune cells remaining poorly understood at the site of *U. urealyticum* infection (after DnaJ-vaccination). Future studies monitoring the recruitment of host immune cells in the uterus during *U. urealyticum* infection could help resolve this issue (Pal et al. 2020; Zhao et al. 2016).

Compared with macrophages, DCs are professional APCs with the ability to bridge innate and adaptive immunity and are necessary for optimal T-cell activation and differentiation (Thomas et al. 2021). Upon sensing inflammatory or infectious stimuli, DCs mature by upregulating co-stimulatory molecules and migrating to the draining lymph node to drive the T-cell

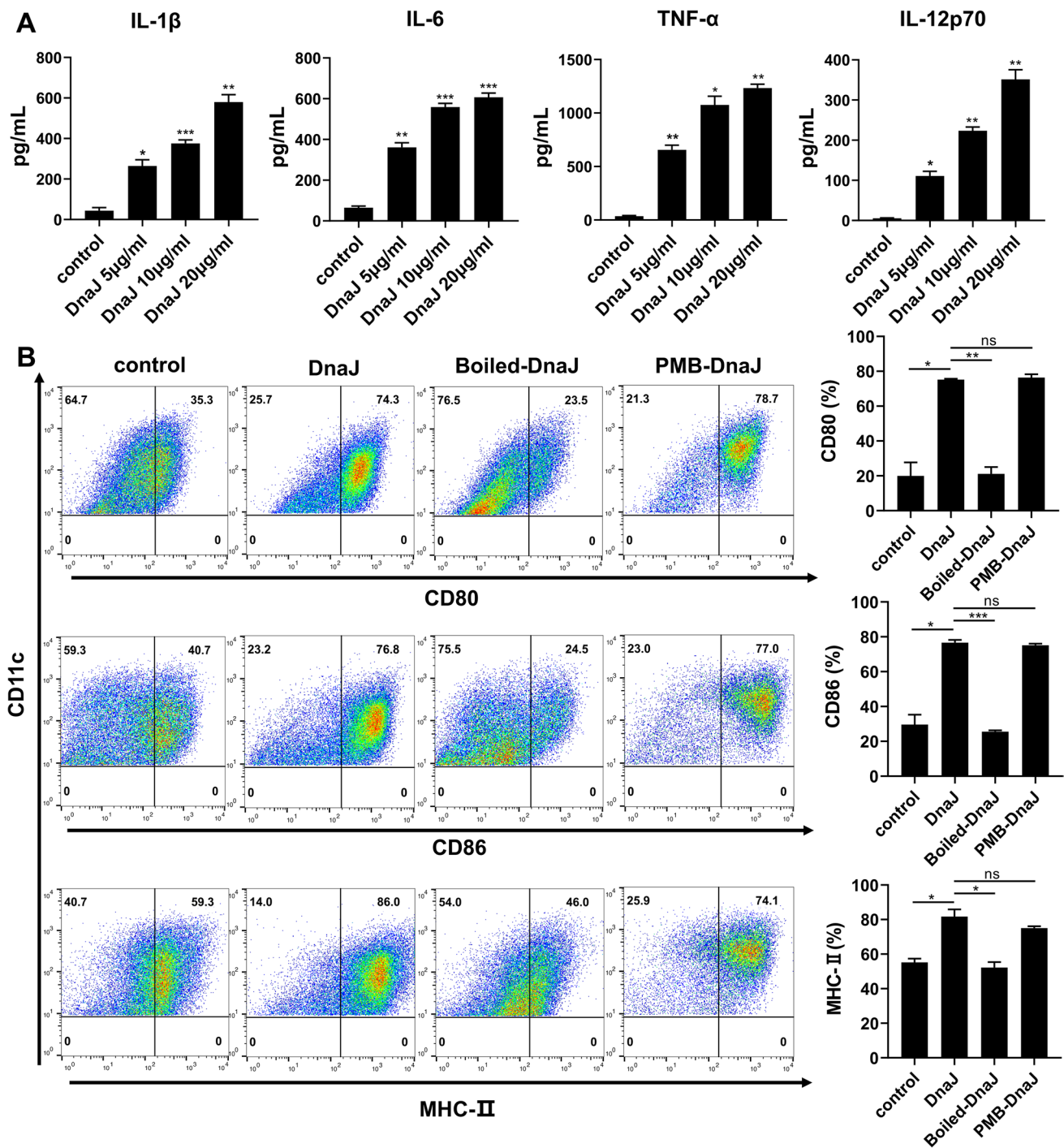


Fig. 8 DnaJ induces BMDCs activation: **A** Immature BMDCs were stimulated with 5–20 μg/mL DnaJ for 24 h. Analysis of IL-1β, IL-6, IL-12p70, and TNF-α production through enzyme-linked immunosorbent assay, **P* < 0.05, ***P* < 0.01 and ****P* < 0.001. Immature BMDCs were treated with 10 μg/mL DnaJ. Alternatively, DCs were stimulated with DnaJ treated with polymyxin B for 3 h at 4 °C or heated at 100 °C for 2 h. After 24 h, the expression of surface mol-

ecules in the cluster of CD11c⁺ BMDCs was measured. **B** Representative plots of CD80, CD86, and MHC-II on BMDCs detected from three independent experiments are shown. Analysis of expression percentages of the surface molecules on BMDCs, **P* < 0.05, ***P* < 0.01, and ns = not significant, *P* > 0.05. The data are representative of three independent experiments

response (Choi et al. 2018). Our analyses of the collected supernatant from the BMDCs activated by DnaJ indicated

that the pro-inflammatory cytokine IL-12p70 levels exhibited a dose-dependent increase. Previous studies on DC-mediated

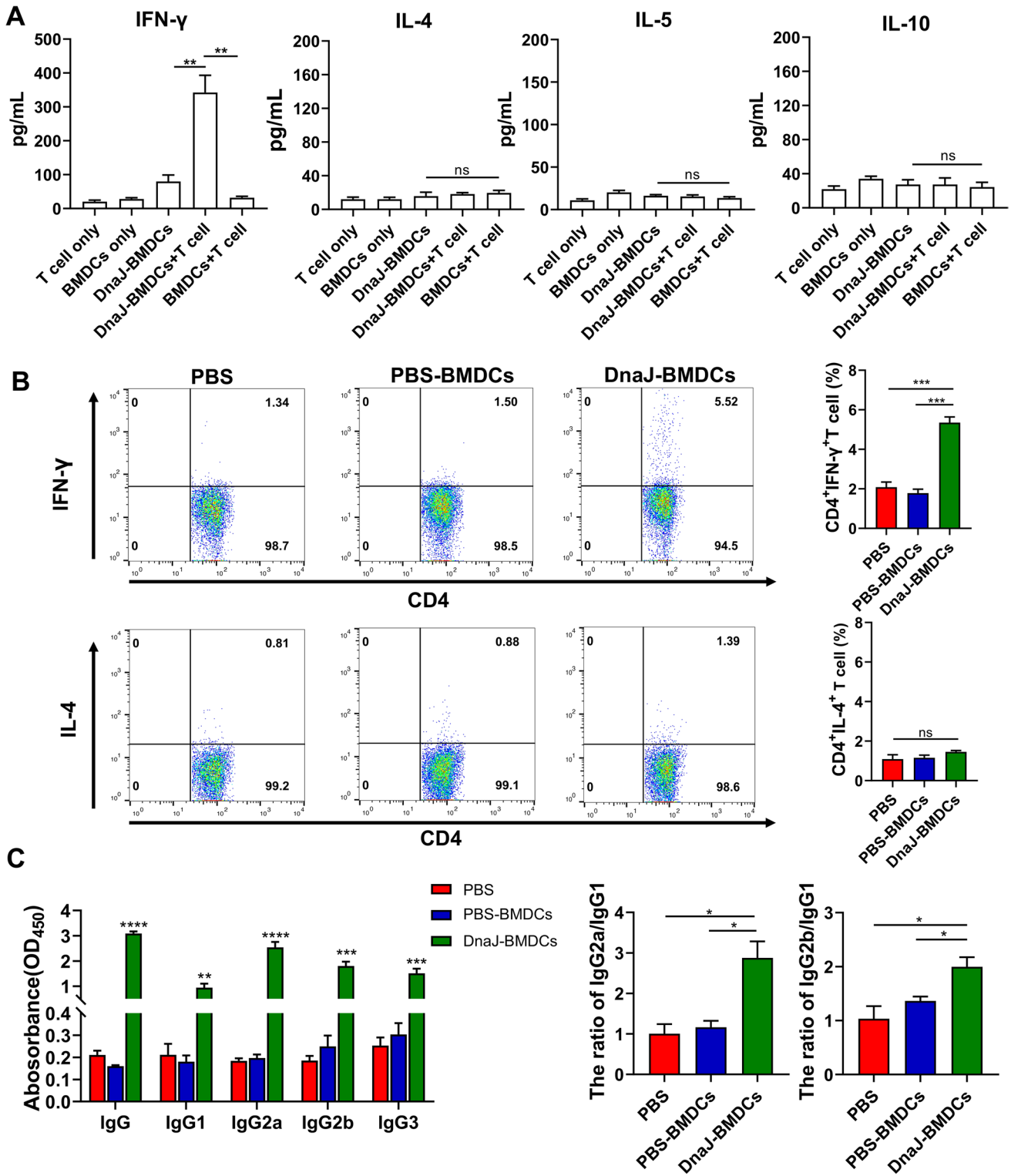


Fig. 9 Regulation of Th1 polarisation by DnaJ via BMDCs modulation: **A** Polarisation of the cluster of differentiation CD4 naïve T cells by DnaJ-treated BMDCs. At 4 days after co-culture, IFN- γ , IL-4, IL-5, and IL-10 levels in the co-culture supernatants were analysed by ELISA, $**P < 0.01$ and ns = not significant, $P > 0.05$. The data are representative of three independent experiments. Immune responses after adoptive immunisation of DnaJ-pulsed BMDCs: **B** The sple-

nocytes from the mice of each group were cultured in DnaJ for 8 h ($n = 4$ mice per group). A flow cytometry assayed the proportion of the activated Th1 cells and Th2 cells in the splenocytes. $***P < 0.001$ and ns = not significant, $P > 0.05$. **C** ELISA of DnaJ-specific IgG subtypes (IgG1, IgG2a, IgG2b, and IgG3) levels in the adoptive immune sera and the calculated IgG2a/IgG1 and IgG2b/IgG1 ratio. $*P < 0.05$, $**P < 0.01$, $***P < 0.001$, and $****P < 0.0001$

IL-12p70 production were critical for initiating an optimal acquired-IFN- γ response from T cells (Barhoumi et al. 2019; Thomas et al. 2021; Varikuti et al. 2021). In BMDC maturation, in addition to the production of cytokines, DnaJ induces BMDCs activation, for example, CD80, CD86, and MHC class II upregulation. Thus, BMDCs maturation by DnaJ treatment may be a key event that induces T-cell responses. This assertion was supported by in vitro studies using BMDC-T cell co-culture. In the co-culture system medium, IFN- γ levels remarkably increased compared with those of the control groups, which showed that DnaJ-stimulated BMDCs potently triggered naïve T cell polarisation towards a Th1 subset. Overall, *U. urealyticum* DnaJ increases BMDCs maturation in a dose-dependent manner and drives the Th1 immune response (Lü et al. 2010).

DCs are crucial for the activation of the host immune system. We have shown that the effect of DnaJ on DCs skews naïve CD4 T cells to Th1-cell differentiation. Interestingly, Shaw et al. (Shaw et al. 2002) indicated that the phenotype and function of ex vivo mature BMDCs may not necessarily predict the immune reactions established in vivo following adoptively transferred cells. In their study, they found that in BMDCs pulsed with *Chlamydia* spp, major outer membrane protein (MOMP) induced CD4 T cells to secrete IFN- γ ex vivo. However, MOMP-pulsed BMDCs adoptive immunisation induced a Th2-rather than a Th1-polarised immune response. To investigate the role of mature BMDCs with DnaJ in Th1 or Th2 polarisation in vivo, mice were immunised with DnaJ-pulsed DCs. We found that Th1 cells were more abundant in the DnaJ-pulsed BMDCs group, whereas no changes in the percentage of Th2 cells in the control groups were observed, which clearly depicted the pro-host immunological properties of this protein antigen. Unlike the mice immunised with DnaJ and Freud's adjuvant, autologous DCs loaded with DnaJ induced a Th1 immune response without bias. We refrained from using an exogenous adjuvant because of its inherent ability to skew the immunological response to vaccine antigens, such as Th1 or Th2 responses (Agger et al. 2008; Arora et al. 2020). Safe and non-toxic adjuvants (including DCs) could induce stronger and more efficacious immune responses when compared to recombinant proteins alone (Ciabattini et al. 2016; Lindblad et al. 1997). However, many challenges in adoptive DCs immunotherapy, such as cost, tedious operation and enough quantity of functional autologous DCs that cannot always be obtained still exist; therefore, finding a desirable adjuvant to synergistically enhance a DnaJ-induced Th1 response rather than a Th2 response, which could provide a promising strategy for developing a safe, inexpensive, and effective *U. urealyticum* vaccine, is necessary (Knudsen et al. 2016).

Supplementary Information The online version contains supplementary material available at <https://doi.org/10.1007/s00253-022-12230-4>.

Author contribution FYG and YHT contributed to study design, literature search, data collection, data analysis and interpretation, figures, and drafting of the manuscript for important intellectual content. WJZ

and HXY contributed to data collection, data interpretation, and critical review of the manuscript. JX and WYT contributed to data interpretation and review of the manuscript. AHL contributed to data analysis and interpretation and review of the manuscript for important intellectual content. GZD and RHL is the guarantor of this work and, as such, had full access to all the data in the study and takes responsibility for the integrity of the data and the accuracy of the data analysis. All authors read and approved the final manuscript.

Funding This work was chiefly supported by funds from the Hunan Provincial Innovation Foundation for Postgraduate (NO. CX20200982), the Research Project of Hunan Provincial Health and Wellness Commission (NO. B2019003), the Hunan Science and Technology Innovation Project (NO. 2018SK50302), the Hunan Provincial Department of Education Project (NO. 19B496) and the Natural Science Foundation of Hunan Province (NO. 2020JJ4521).

Data availability The datasets generated during and/or analysed during the current study are available from the corresponding author upon reasonable request.

Code availability Not applicable.

Declarations

Ethics approval All protocols were approved by the Institutional Animal Care and Use Committee of the University of South China (approval number USC202009XS07).

Consent to participate Not applicable.

Consent for publication Not applicable.

Conflict of interest The authors declare no competing interests.

References

- Abbas G, Zafar I, Ahmad S, Azam SS (2020) Immunoinformatics design of a novel multi-epitope peptide vaccine to combat multi-drug resistant infections caused by *Vibrio vulnificus*. Eur J Pharm Sci 142:105160. <https://doi.org/10.1016/j.ejps.2019.105160>
- Agger EM, Cassidy JP, Brady J, Korsholm KS, Vingsbo-Lundberg C, Andersen P (2008) Adjuvant modulation of the cytokine balance in *Mycobacterium tuberculosis* subunit vaccines; immunity, pathology and protection. Immunology 124(2):175–185. <https://doi.org/10.1111/j.1365-2567.2007.02751.x>
- Akache B, Agbayani G, Stark FC, Jia Y, Dudani R, Harrison BA, Deschatelets L, Chandan V, Lam E, Hemraz UD, Régnier S, Krishnan L, McCluskie MJ (2021) Sulfated Lactosyl Archaeol Archaeosomes Synergize with Poly(I:C) to Enhance the Immunogenicity and Efficacy of a Synthetic Long Peptide-based Vaccine in a Melanoma Tumor Model. Pharmaceutics 13(2). <https://doi.org/10.3390/pharmaceutics13020257>
- Arora SK, Alam A, Naqvi N, Ahmad J, Sheikh JA, Rahman SA, Hasnain SE, Ehtesham NZ (2020) Immunodominant *Mycobacterium tuberculosis* Protein Rv1507A Elicits Th1 Response and Modulates Host Macrophage Effector Functions. Front Immunol 11:1199. <https://doi.org/10.3389/fimmu.2020.01199>
- Back YW, Bae HS, Choi HG, Binh DT, Son YJ, Choi S, Kim HJ (2020) Fusion of Dendritic Cells Activating Rv2299c Protein Enhances the Protective Immunity of Ag85B-ESAT6 Vaccine Candidate against *Tuberculosis*. Pathogens 9(11). <https://doi.org/10.3390/pathogens9110865>

- Barhoumi M, Koutsoni OS, Dotsika E, Guizani I (2019) *Leishmania infantum* LeIF and its recombinant polypeptides induce the maturation of dendritic cells in vitro: An insight for dendritic cells based vaccine. *Immunol Lett* 210:20–28. <https://doi.org/10.1016/j.imlet.2019.04.001>
- Bebear CM, Renaudin H, Charron A, Gruson D, Lefrancois M, Bebear C (2000) In vitro activity of trovafloxacin compared to those of five antimicrobials against mycoplasmas including *Mycoplasma hominis* and *Ureaplasma urealyticum* fluoroquinolone-resistant isolates that have been genetically characterized. *Antimicrob Agents Chemother* 44(9):2557–2560. <https://doi.org/10.1128/aac.44.9.2557-2560.2000>
- Bollyky PL, Evanko SP, Wu RP, Potter-Perigo S, Long SA, Kinsella B, Reijonen H, Guebtner K, Teng B, Chan CK, Braun KR, Gebe JA, Nepom GT, Wight TN (2010) Th1 cytokines promote T-cell binding to antigen-presenting cells via enhanced hyaluronan production and accumulation at the immune synapse. *Cell Mol Immunol* 7(3):211–220. <https://doi.org/10.1038/cmi.2010.9>
- Bracher A, Verghese J (2015) GrpE, Hsp110/Grp170, HspBP1/Sil1 and BAG domain proteins: nucleotide exchange factors for Hsp70 molecular chaperones. *Subcell Biochem* 78:1–33. https://doi.org/10.1007/978-3-319-11731-7_1
- Brunham RC, Rappuoli R (2013) *Chlamydia trachomatis* control requires a vaccine. *Vaccine* 31(15):1892–1897. <https://doi.org/10.1016/j.vaccine.2013.01.024>
- Choi S, Choi HG, Lee J, Shin KW, Kim HJ (2018) *Mycobacterium tuberculosis* protein Rv2220 induces maturation and activation of dendritic cells. *Cell Immunol* 328:70–78. <https://doi.org/10.1016/j.cellimm.2018.03.012>
- Ciabattini A, Pettini E, Fiorino F, Pastore G, Andersen P, Pozzi G, Medaglini D (2016) Modulation of primary immune response by different vaccine adjuvants. *Front Immunol* 7:427. <https://doi.org/10.3389/fimmu.2016.00427>
- Colaco CA, Bailey CR, Walker KB, Keeble J (2013) Heat shock proteins: stimulators of innate and acquired immunity. *Biomed Res Int* 2013:461230. <https://doi.org/10.1155/2013/461230>
- Dai G, Li R, Chen H, Jiang C, You X, Wu Y (2015) A ferritin-like protein with antioxidant activity in *Ureaplasma urealyticum*. *BMC Microbiol* 15:145. <https://doi.org/10.1186/s12866-015-0485-6>
- Eslamizar L, Petrovas C, Leggat DJ, Furr K, Lifton ML, Levine G, Ma S, Fletez-Brant C, Hoyland W, Prabhakaran M, Narpala S, Boswell K, Yamamoto T, Liao HX, Pickup D, Ramsburg E, Sutherland L, McDermott A, Roederer M, Montefiori D, Koup RA, Haynes BF, Letvin NL, Santra S (2021) Recombinant MVA-prime elicits neutralizing antibody responses by inducing antigen-specific B cells in the germinal center. *NPJ Vaccines* 6(1):15. <https://doi.org/10.1038/s41541-020-00277-1>
- Fang L, Sun L, Yang J, Gu Y, Zhan B, Huang J, Zhu X (2014) Heat shock protein 70 from *Trichinella spiralis* induces protective immunity in BALB/c mice by activating dendritic cells. *Vaccine* 32(35):4412–4419. <https://doi.org/10.1016/j.vaccine.2014.06.055>
- Farris CM, Morrison SG, Morrison RP (2010) CD4+ T cells and antibody are required for optimal major outer membrane protein vaccine-induced immunity to *Chlamydia muridarum* genital infection. *Infect Immun* 78(10):4374–4383. <https://doi.org/10.1128/iai.00622-10>
- Geng R, Ren Y, Rao R, Tan X, Zhou H, Yang X, Liu W, Lu Q (2020) Titanium dioxide nanoparticles induced HeLa cell necrosis under UVA radiation through the ROS-mPTP Pathway. *Nanomaterials (Basel)* 10(10). <https://doi.org/10.3390/nano10102029>
- Glass JI, Lefkowitz EJ, Glass JS, Heiner CR, Chen EY, Cassell GH (2000) The complete sequence of the mucosal pathogen *Ureaplasma urealyticum*. *Nature* 407(6805):757–762. <https://doi.org/10.1038/35037619>
- Gold MC, Ehlinger HD, Cook MS, Smyk-Pearson SK, Wille PT, Ungerleider RM, Lewinsohn DA, Lewinsohn DM (2008) Human innate *Mycobacterium tuberculosis*-reactive alphabetaTCR+ thymocytes. *PLoS Pathog* 4(2):e39. <https://doi.org/10.1371/journal.ppat.0040039>
- Goldenberg RL, Andrews WW, Goepfert AR, Faye-Petersen O, Cliver SP, Carlo WA, Hauth JC (2008) The Alabama Preterm Birth Study: umbilical cord blood *Ureaplasma urealyticum* and *Mycoplasma hominis* cultures in very preterm newborn infants. *Am J Obstet Gynecol* 198(1):43.e1–5. <https://doi.org/10.1016/j.ajog.2007.07.033>
- Grifoni A, Sidney J, Zhang Y, Scheuermann RH, Peters B, Sette A (2020) A sequence homology and bioinformatic approach can predict candidate targets for immune responses to SARS-CoV-2. *Cell Host Microbe* 27(4):671–680.e2. <https://doi.org/10.1016/j.chom.2020.03.002>
- Inaba K, Inaba M, Romani N, Aya H, Deguchi M, Ikehara S, Muramatsu S, Steinman RM (1992) Generation of large numbers of dendritic cells from mouse bone marrow cultures supplemented with granulocyte/macrophage colony-stimulating factor. *J Exp Med* 176(6):1693–1702. <https://doi.org/10.1084/jem.176.6.1693>
- Iwasaka T, Wada T, Kidera Y, Sugimori H (1986) Hormonal status and *mycoplasma* colonization in the female genital tract. *Obstet Gynecol* 68(2):263–266
- Jumper J, Evans R, Pritzel A, Green T, Figurnov M, Ronneberger O, Tunyasuvunakool K, Bates R, Židek A, Potapenko A, Bridgland A, Meyer C, Kohl SAA, Ballard AJ, Cowie A, Romera-Paredes B, Nikolov S, Jain R, Adler J, Back T, Petersen S, Reiman D, Clancy E, Zielinski M, Steinegger M, Pacholska M, Berghammer T, Bodenstein S, Silver D, Vinyals O, Senior AW, Kavukcuoglu K, Kohli P, Hassabis D (2021) Highly accurate protein structure prediction with AlphaFold. *Nature* 596(7873):583–589. <https://doi.org/10.1038/s41586-021-03819-2>
- Kim WS, Jung ID, Kim JS, Kim HM, Kwon KW, Park YM, Shin SJ (2018) *Mycobacterium tuberculosis* GrpE, A heat-shock stress responsive chaperone, promotes Th1-biased T cell immune response via TLR4-mediated activation of dendritic cells. *Front Cell Infect Microbiol* 8:95. <https://doi.org/10.3389/fcimb.2018.00095>
- Knudsen NP, Olsen A, Buonsanti C, Follmann F, Zhang Y, Coler RN, Fox CB, Meinke A, D'Oro U, Casini D, Bonci A, Billeskov R, De Gregorio E, Rappuoli R, Harandi AM, Andersen P, Agger EM (2016) Different human vaccine adjuvants promote distinct antigen-independent immunological signatures tailored to different pathogens. *Sci Rep* 6:19570. <https://doi.org/10.1038/srep19570>
- Kokkayil P, Dhawan B (2015) *Ureaplasma*: current perspectives. *Indian J Med Microbiol* 33(2):205–214. <https://doi.org/10.4103/0255-0857.154850>
- Li P, Liu Q, Luo H, Liang K, Han Y, Roland KL, Curtiss R 3rd, Kong Q (2018) Bi-valent polysaccharides of Vi capsular and O9 O-antigen in attenuated *Salmonella Typhimurium* induce strong immune responses against these two antigens. *NPJ Vaccines* 3:1. <https://doi.org/10.1038/s41541-017-0041-5>
- Li Y, Zheng K, Tan Y, Wen Y, Wang C, Chen Q, Yu J, Xu M, Tan M, Wu Y (2019) A recombinant multi-epitope peptide vaccine based on MOMP and CPSIT_p6 protein protects against *Chlamydia psittaci* lung infection. *Appl Microbiol Biotechnol* 103(2):941–952. <https://doi.org/10.1007/s00253-018-9513-4>
- Lindblad EB, Elhay MJ, Silva R, Appelberg R, Andersen P (1997) Adjuvant modulation of immune responses to *tuberculosis* subunit vaccines. *Infect Immun* 65(2):623–629. <https://doi.org/10.1128/iai.65.2.623-629.1997>
- Liu J, Du S, Kong Q, Zhang X, Jiang S, Cao X, Li Y, Li C, Chen H, Ding Z, Liu L (2020) HSPA12A attenuates lipopolysaccharide-induced liver injury through inhibiting caspase-11-mediated hepatocyte pyroptosis via PGC-1 α -dependent acylxyacyl hydrolase expression. *Cell Death Differ* 27(9):2651–2667. <https://doi.org/10.1038/s41418-020-0536-x>

- Lü H, Wang H, Zhao HM, Zhao L, Chen Q, Qi M, Liu J, Yu H, Yu XP, Yang X, Zhao WM (2010) Dendritic cells (DCs) transfected with a recombinant adenovirus carrying chlamydial major outer membrane protein antigen elicit protective immune responses against genital tract challenge infection. *Biochem Cell Biol* 88(4):757–765. <https://doi.org/10.1139/o10-011>
- Matsui HM, Hazama S, Nakajima M, Xu M, Matsukuma S, Tokumitsu Y, Shindo Y, Tomochika S, Yoshida S, Iida M, Suzuki N, Takeda S, Yoshino S, Ueno T, Oka M, Nagano H (2021) Novel adjuvant dendritic cell therapy with transfection of heat-shock protein 70 messenger RNA for patients with hepatocellular carcinoma: a phase I/II prospective randomized controlled clinical trial. *Cancer Immunol Immunother* 70(4):945–957. <https://doi.org/10.1007/s00262-020-02737-y>
- Noh EJ, Kim DJ, Lee JY, Park JH, Kim JS, Han JW, Kim BC, Kim CJ, Lee SK (2019) *Ureaplasma Urealyticum* infection contributes to the development of pelvic endometriosis through toll-like receptor 2. *Front Immunol* 10:2373. <https://doi.org/10.3389/fimmu.2019.02373>
- Noya V, Brossard N, Rodríguez E, Dergan-Dylon LS, Carmona C, Rabinovich GA, Freire T (2017) A mucin-like peptide from *Fasciola hepatica* instructs dendritic cells with parasite specific Th1-polarizing activity. *Sci Rep* 7:40615. <https://doi.org/10.1038/srep40615>
- Pal S, Cruz-Fisher MI, Cheng C, Carmichael JR, Tifrea DF, Tatarenkova O, de la Maza LM (2020) Vaccination with the recombinant major outer membrane protein elicits long-term protection in mice against vaginal shedding and infertility following a *Chlamydia muridarum* genital challenge. *NPJ Vaccines* 5:90. <https://doi.org/10.1038/s41541-020-00239-7>
- Paul S, Lindestam Arlehamn CS, Scriba TJ, Dillon MB, Oseroff C, Hinz D, McKinney DM, Carrasco Pro S, Sidney J, Peters B, Sette A (2015) Development and validation of a broad scheme for prediction of HLA class II restricted T cell epitopes. *J Immunol Methods* 422:28–34. <https://doi.org/10.1016/j.jim.2015.03.022>
- Qin L, Chen Y, You X (2019) Subversion of the Immune Response by Human Pathogenic *Mycoplasmas*. *Front Microbiol* 10:1934. <https://doi.org/10.3389/fmicb.2019.01934>
- Reyes L, Reinhard M, Brown MB (2009) Different inflammatory responses are associated with *Ureaplasma parvum*-induced UTI and urolith formation. *BMC Infect Dis* 9:9. <https://doi.org/10.1186/1471-2334-9-9>
- Rittenschöber-Böhm J, Waldhoer T, Schulz SM, Stihsen B, Pimpel B, Goeral K, Hafner E, Sliutz G, Kasper DC, Witt A, Berger A (2018) First trimester vaginal *Ureaplasma* biovar colonization and preterm birth: results of a prospective multicenter study. *Neonatology* 113(1):1–6. <https://doi.org/10.1159/000480065>
- Sen-Kilic E, Blackwood CB, Boehm DT, Witt WT, Malkowski AC, Bevere JR, Wong TY, Hall JM, Bradford SD, Varney ME, Dameron FH, Barbier M (2019) Intranasal peptide-based FpvA-KLH conjugate vaccine protects mice From *Pseudomonas aeruginosa* Acute Murine Pneumonia. *Front Immunol* 10:2497. <https://doi.org/10.3389/fimmu.2019.02497>
- Shaw J, Grund V, Durling L, Crane D, Caldwell HD (2002) Dendritic cells pulsed with a recombinant *chlamydial* major outer membrane protein antigen elicit a CD4(+) type 2 rather than type 1 immune response that is not protective. *Infect Immun* 70(3):1097–1105. <https://doi.org/10.1128/iai.70.3.1097-1105.2002>
- Shiragannavar SJ, Madagi SB (2021) Identification of vaccine candidate proteins in *Ureaplasma urealyticum* causing infertility. *Indian J Sex Transm Dis AIDS* 42(2):95–100. https://doi.org/10.4103/ijstd.IJSTD_7_19
- Silwedel C, Speer CP, Härtel C, Glaser K (2020) *Ureaplasma*-driven neuroinflammation in neonates: assembling the Puzzle Pieces. *Neonatology* 117(6):665–672. <https://doi.org/10.1159/000512019>
- Sprong KE, Mabenge M, Wright CA, Govender S (2020) *Ureaplasma species* and preterm birth: current perspectives. *Crit Rev Microbiol* 46(2):169–181. <https://doi.org/10.1080/1040841x.2020.1736986>
- Sweeney EL, Dando SJ, Kallapur SG, Knox CL (2017) The human *Ureaplasma Species* as causative agents of chorioamnionitis. *Clin Microbiol Rev* 30(1):349–379. <https://doi.org/10.1128/cmr.00091-16>
- Tang Y, Guo F, Lei A, Xiang J, Liu P, Ten W, Dai G, Li R (2020) GrpE Immunization Protects Against *Ureaplasma urealyticum* Infection in BALB/C Mice. *Front Immunol* 11:1495. <https://doi.org/10.3389/fimmu.2020.01495>
- Taylor-Robinson D (2017) Mollicutes in vaginal microbiology: *Mycoplasma hominis*, *Ureaplasma urealyticum*, *Ureaplasma parvum* and *Mycoplasma genitalium*. *Res Microbiol* 168(9–10):875–881. <https://doi.org/10.1016/j.resmic.2017.02.009>
- Thomas R, Wang S, Shekhar S, Peng Y, Qiao S, Zhang C, Shan L, Movassagh H, Gounni AS, Yang J, Yang X (2021) Semaphorin 3E protects against *Chlamydia* infection by modulating dendritic cell functions. *J Immunol* 206(6):1251–1265. <https://doi.org/10.4049/jimmunol.2001013>
- Triantafilou M, De Glanville B, Aboklaish AF, Spiller OB, Kotecha S, Triantafilou K (2013) Synergic activation of toll-like receptor (TLR) 2/6 and 9 in response to *Ureaplasma parvum* & *urealyticum* in human amniotic epithelial cells. *PLoS ONE* 8(4):e61199. <https://doi.org/10.1371/journal.pone.0061199>
- Varikuti S, Verma C, Natarajan G, Oghumu S, Satoskar AR (2021) MicroRNA155 plays a critical role in the pathogenesis of cutaneous *Leishmania* major infection by promoting a Th2 response and attenuating dendritic cell activity. *Am J Pathol* 191(5):809–816. <https://doi.org/10.1016/j.ajpath.2021.01.012>
- Viscardi RM, Kaplan J, Lovchik JC, He JR, Hester L, Rao S, Hasday JD (2002) Characterization of a murine model of *Ureaplasma urealyticum* pneumonia. *Infect Immun* 70(10):5721–5729. <https://doi.org/10.1128/iai.70.10.5721-5729.2002>
- Waites KB, Crabb DM, Xiao L, Duffy LB, Leal SM, Jr. (2020) In vitro activities of eravacycline and other antimicrobial agents against human *Mycoplasmas* and *Ureaplasmas*. *Antimicrob Agents Chemother* 64(8). <https://doi.org/10.1128/aac.00698-20>
- Yang T, Pan L, Wu N, Wang L, Liu Z, Kong Y, Ruan Z, Xie X, Zhang J (2020) Antimicrobial Resistance in Clinical *Ureaplasma* spp. and *Mycoplasma hominis* and Structural Mechanisms Underlying Quinolone Resistance. *Antimicrob Agents Chemother* 64(6). <https://doi.org/10.1128/aac.02560-19>
- Ye L, Jiang Y, Yang G, Yang W, Hu J, Cui Y, Shi C, Liu J, Wang C (2017) Murine bone marrow-derived DCs activated by *porcine rotavirus* stimulate the Th1 subtype response in vitro. *Microb Pathog* 110:325–334. <https://doi.org/10.1016/j.micpath.2017.07.015>
- Zhao J, Zhao J, Mangalam AK, Channappanavar R, Fett C, Meyerholz DK, Agnihotram S, Baric RS, David CS, Perlman S (2016) Airway memory CD4(+) T cells mediate protective immunity against emerging *Respiratory Coronaviruses*. *Immunity* 44(6):1379–1391. <https://doi.org/10.1016/j.immuni.2016.05.006>
- Zügel U, Kaufmann SH (1999) Immune response against heat shock proteins in infectious diseases. *Immunobiology* 201(1):22–35. [https://doi.org/10.1016/s0171-2985\(99\)80044-8](https://doi.org/10.1016/s0171-2985(99)80044-8)

Publisher's note Springer Nature remains neutral with regard to jurisdictional claims in published maps and institutional affiliations.

Springer Nature or its licensor (e.g. a society or other partner) holds exclusive rights to this article under a publishing agreement with the author(s) or other rightsholder(s); author self-archiving of the accepted manuscript version of this article is solely governed by the terms of such publishing agreement and applicable law.